Title

3′-Deoxy-3′-18F-Fluorothymidine PET and MRI for Early Survival Predictions in Patients with Recurrent Malignant Glioma Treated with Bevacizumab

Permalink

https://escholarship.org/uc/item/2nn2q9kt

Journal

Journal of Nuclear Medicine, 53(1)

ISSN

0161-5505

Authors

Schwarzenberg, Johannes
Czernin, Johannes
Cloughesy, Timothy F
et al.

Publication Date

2012

DOI

10.2967/jnumed.111.092387

Peer reviewed

3′-Deoxy-3′-18F-Fluorothymidine PET and MRI for Early Survival Predictions in Patients with Recurrent Malignant Glioma Treated with Bevacizumab

Johannes Schwarzenberg[1,2,3], **Johannes Czernin**[1,2], **Timothy F. Cloughesy**[4], **Benjamin M. Ellingson**[5], **Whitney B. Pope**[5], **Cheri Geist**[1,2], **Magnus Dahlbom**[1,2], **Daniel H.S. Silverman**[1,2], **Nagichettiar Satyamurthy**[1], **Michael E. Phelps**[1], and **Wei Chen**[1,2]

[1]Department of Molecular and Medical Pharmacology, University of California, Los Angeles, California

[2]Ahmanson Translational Imaging Division, University of California, Los Angeles, California

[3]Department of Pediatric and Adolescent Medicine, Medical University of Vienna, Vienna, Austria

[4]Department of Neurology, University of California, Los Angeles, California

[5]Department of Radiological Sciences, University of California, Los Angeles, California

Abstract

With the dismal prognosis for malignant glioma patients, survival predictions become key elements in patient management. This study compares the value of 3′-deoxy-3′-18F-fluorothymidine (18F-FLT) PET and MRI for early outcome predictions in patients with recurrent malignant glioma on bevacizumab therapy.

Methods—Thirty patients treated with bevacizumab combination therapy underwent 18F-FLT PET immediately before and at 2 and 6 wk after the start of treatment. A metabolic treatment response was defined as a decrease of equal to or greater than 25% in tumor 18F-FLT uptake (standardized uptake values) from baseline using receiver-operating-characteristic analysis. MRI treatment response was assessed at 6 wk according to the Response Assessment in Neurooncology criteria. 18F-FLT responses at different times were compared with MRI response and correlated with progression-free survival and overall survival using Kaplan–Meier analysis. Metabolic response based on 18F-FLT was further compared with other outcome predictors using Cox regression analysis.

Results—Early and late changes in tumor 18F-FLT uptake were more predictive of overall survival than MRI criteria ($P < 0.001$ and $P = 0.01$, respectively). 18F-FLT uptake changes were also predictive of progression-free survival ($P < 0.001$). The median overall survival for responders was 3.3 times longer than for nonresponders based on 18F-FLT PET criteria (12.5 vs. 3.8 mo, $P < 0.001$) but only 1.4 times longer using MRI assessment (12.9 vs. 9.0 mo, $P = 0.05$). On the basis of the 6-wk 18F-FLT PET response, there were 16 responders (53%) and 14 nonresponders (47%), whereas MRI identified 9 responders (7 partial response, 2 complete response, 31%) and 20 nonresponders (13 stable disease, 7 progressive disease, 69%). In 7 of the 8 discrepant cases between MRI and PET, 18F-FLT PET was able to demonstrate response earlier

than MRI. Among various outcome predictors, multivariate analysis identified ^{18}F-FLT PET changes at 6 wk as the strongest independent survival predictor ($P < 0.001$; hazard ratio, 10.051).

Conclusion—Changes in tumor ^{18}F-FLT uptake were highly predictive of progression-free and overall survival in patients with recurrent malignant glioma on bevacizumab therapy. ^{18}F-FLT PET seems to be more predictive than MRI for early treatment response.

Keywords

^{18}F-FLT PET; bevacizumab; malignant glioma; survival prediction

---

Malignant gliomas are aggressive primary brain tumors that almost always lead to rapid patient deterioration and death (1,2). Bevacizumab (Avastin; Genentec) is a recombinant humanized monoclonal antibody targeting vascular endothelial growth factor, a protein released by tumor cells to recruit novel blood vessels to support tumor growth (3,4). Treatment with bevacizumab has resulted in 6-mo progression-free survival (PFS) rates of 46% for patients with recurrent glioblastomas (5), a significant improvement when compared with historical data that showed 6-mo PFS of 9%–21% (1,6–8). Improvement in PFS and overall survival (OS) was also shown in 61 patients with recurrent high-grade glioma (9). In a multicenter study, 167 patients with glioblastoma were randomly assigned to receive bevacizumab alone or bevacizumab in combination with irinotecan. Six-month PFS rates of 42.6% for bevacizumab only and 50.3% for bevacizumab combined with irinotecan were observed (10).

Classic glioma treatment response assessment (Macdonald criteria) is based on 2-dimensional MRI contrast-enhancing tumor area changes as the primary measure while considering the use of steroids and changes in the neurologic status (11). It has been recognized that MRI contrast enhancement primarily reflects a disrupted blood–brain barrier, which can be influenced by changes in corticosteroid dose as well as other treatment effects such as inflammation, radiation necrosis, and postsurgical change (12,13). In addition, it was recognized that nonenhancing T2-weighted and fluid-attenuated inversion recovery sequence changes can reflect tumor recurrence as well, especially in patients on antiangiogenic therapy (13,14). Thus, it has been proposed by the recently published Response Assessment in Neurooncology (RANO) that changes in both enhancing and nonenhancing areas should be considered in evaluating treatment response by MRI (14,15).

PET with ^{18}F-FDG directly reflects the glucose metabolic activity of tumor cells and is predictive of patient outcome (16,17). However, variability of glucose uptake in recurrent high-grade gliomas and low tumor-to-background ratios due to the high metabolic activity of healthy brain tissue limit the usefulness of ^{18}F-FDG PET (18).

3′-deoxy-3′-^{18}F-fluorothymidine (^{18}F-FLT) is a thymidine analog that has been developed to image tumor cell proliferation (19). A pilot study in 19 patients with recurrent high-grade glioma has previously shown that ^{18}F-FLT uptake can be used to identify responders and nonresponders on a bevacizumab and irinotecan regimen (20). ^{18}F-FLT uptake change was not significant in predicting PFS in that study, although a trend was observed.

The current report presents the completed study on the value of ^{18}F-FLT PET for predicting both PFS and OS in an expanded study population of 30 patients with recurrent high-grade glioma who underwent treatment with bevacizumab combination therapy. The predictive power of ^{18}F-FLT tumor uptake was also compared with outcome predictions derived from MRI according to the RANO criteria.

MATERIALS AND METHODS

Patients

Thirty patients with recurrent high-grade glioma were enrolled in this study (Table 1). There were 18 men and 12 women, with a median age of 58 y. All patients met the following inclusion criteria. Patients had a histologically confirmed diagnosis of glioblastoma or anaplastic astrocytoma (glioblastoma, $n = 24$; anaplastic astrocytoma, $n = 6$) and had previously undergone surgical resection and chemoradiation therapy. All had MRI-confirmed recurrent disease by the time bevacizumab treatment was started. Further criteria included a Karnofsky performance score (KPS) of 70 or greater, adequate hematologic values, and sufficient hepatic and renal function. Patients were excluded if there was a bleeding disorder, a recent history of intracranial bleeding, or thromboembolism.

All patients gave written consent to participate in this study, which had been approved by the University of California, Los Angeles, Office for Protection of Research Subjects.

Treatment

All patients were treated with bevacizumab and irinotecan except for 3 patients who were treated with bevacizumab alone (patients 24, 27, and 29, Table 1). Treatment was discontinued when patients experienced clinical or radiographic disease progression. The coadministration of corticosteroids was closely monitored. Although 12 patients did not require corticosteroids, 10 patients were maintained on stable or tapering doses of dexamethasone, and 8 patients needed a dose increase after the baseline MRI and PET studies were obtained.

Patients' disease status was evaluated and monitored using gadolinium-enhanced and nonenhanced MRI within 1 wk before and at approximately 6-wk intervals after starting bevacizumab treatment. All patients were followed until death. Thus, the outcome data are complete. The OS was defined as the interval between treatment initiation and death, and PFS was defined as the interval between treatment initiation and radiographic or clinical progression. No patient was lost to follow-up.

PET

^{18}F-FLT was synthesized locally as has been previously described (21). A baseline ^{18}F-FLT PET scan was obtained for all patients within 3 ± 2 d before treatment initiation, and follow-up ^{18}F-FLT PET was performed at 2 and 6 wk after treatment initiation. All images were obtained using a high-resolution full-ring PET scanner (ECAT HR+; Siemens/CTI) capable of simultaneous registration of 63 contiguous slices.

Patients were instructed to drink ample amounts of water before the scan to facilitate tracer excretion. Immediately after intravenous injection of ^{18}F-FLT (2.0 MBq/kg), a transmission scan was obtained for attenuation correction, followed by a 60-min dynamic emission acquisition sequence in 3-dimensional mode.

The data were reconstructed using iterative ordered-subset expectation maximization (8 iterations with 6 subsets) and a gaussian filter of 5 mm in full width at half maximum using the measured attenuation correction, with consecutive quadratic matrices of 128×128 mm made of cubic voxels of 2.4-mm dimension. The emission data from 30 to 60 min were summed to obtain a region of interest (ROI) and determine the standardized uptake values (SUV). The slice with the highest SUV and the 2 adjacent slices were typically included in the ROI analysis. A circular ROI (diameter, 1.0 cm; 16 pixels) was placed over the hottest

region in the tumor, and mean SUV of this ROI was used in the ^{18}F-FLT PET uptake analysis.

MRI

Data were collected on a 1.5-T MRI system (GE Healthcare) using pulse sequences supplied by the scanner manufacturer. Standard anatomic MRI sequences included axial proton density, T1-, and T2-weighted fast spin-echo images and fluid-attenuated inversion recovery images, all obtained with a 5-mm slice thickness with 1-mm interslice distance, 2 excitations, a matrix of 256×256, and a field of view of 24 cm. Additionally, gadopentetate dimeglumine–enhanced (Magnevist [Berle]; 0.1 mmol/kg) axial and coronal T1-weighted images were acquired after contrast injection.

MRI Response Assessment

Regions of fluid-attenuated inversion recovery abnormality were chosen using RANO recommendations (14). The regions of postcontrast T1-weighted image (T1+C) hyperintensity were defined, excluding any T1 shortening from blood products on precontrast T1-weighted images and cystic and surgical resection cavities. The volumes of fluid-attenuated inversion recovery and T1+C were calculated using a semiautomated procedure as described previously (15).

MRI-based response at 6 wk was defined according to the RANO criteria. However, the 4-wk sustained response requirement for complete response (CR) and partial response (PR) was not considered because the goal of the study was to compare the predictive values of MRI and PET at 6 wk after starting treatment (14). Progressive disease (PD) was defined as more than a 25% increase in the sum of the products of perpendicular diameters, a significant increase in nonenhancing tumor, or neurologic decline. CR was defined as no enhancing or nonenhancing tumor, with no steroids. PR was defined as more than a 50% decrease in the sum of the products of perpendicular diameters on stable steroids without new lesions. Nonenhancing tumor was identified by mass effect or architectural distortion including blurring of the gray–white interface. MRI assessment was performed by a board-certified neuroradiologist.

Statistical Analysis

Differences between groups of patients were established by the *t* test. On the basis of previous studies, a reduction of 25% or greater in ^{18}F-FLT tumor uptake changes was considered a metabolic response (20). This was further verified using receiver-operating-characteristic curve analysis.

Kaplan–Meier curves were subsequently generated to obtain survival estimates (22). Statistical analyses of multiple variables were performed with the Cox proportional hazards model (23). Variables reaching a significance of *P* less than 0.05 by univariate analysis were included in the multivariate analysis.

RESULTS

^{18}F-FLT PET Uptake Changes

Thirty patients were registered for the ^{18}F-FLT PET study between June 2005 and February 2007 (Table 1). All 30 patients completed the baseline scan and the follow-up ^{18}F-FLT PET scan 2 wk later. Twenty-seven patients were able to complete the third ^{18}F-FLT PET scan 6 wk after starting treatment. Rapid clinical deterioration or death prevented 3 patients from undergoing this third ^{18}F-FLT PET scan.

Tumor SUVs and their changes between scans were calculated (Table 2). Mean tumor SUV on baseline scans varied between 0.38 and 4.79, reflecting potentially the heterogeneity in proliferative activity of recurrent high-grade brain tumors. For all patients, the median change of ^{18}F-FLT uptake was −31% at 2 wk, −33% at 6 wk, and +5% between 2 and 6 wk. Examples of individual responses are shown in Figure 1. Essentially all patients showed an initial decrease in ^{18}F-FLT uptake at 2 wk. This decrease was followed by 2 main patterns at 6 wk, either a sustained low ^{18}F-FLT uptake or a rebound of ^{18}F-FLT uptake toward the baseline level (Fig. 2).

Optimal ^{18}F-FLT PET Criteria for Survival Prediction

Absolute uptake values of ^{18}F-FLT (at baseline, 2 wk, or 6 wk) were initially analyzed but were found not to be predictive of survival. Comparing baseline with 2 wk, baseline with 6 wk, and 2 wk with 6 wk, 3 datasets of ^{18}F-FLT tumor uptake values were generated and analyzed in the context of overall patient survival. Using receiver-operating-characteristic analysis, we found the optimal threshold value for ^{18}F-FLT SUV change between baseline and the 6-wk follow-up to be at 25% FLT uptake decrease (area under the curve, 0.779; $P =$ 0.017), resulting in a sensitivity and specificity of 82% and 80%, respectively.

^{18}F-FLT tumor uptake changes at both 2 and 6 wk were significant predictors of OS by Kaplan–Meier analysis ($P < 0.001$; Fig. 3). However, the ^{18}F-FLT tumor response at 6 wk was most predictive for patient outcome according to the Cox regression analysis. On the basis of ^{18}F-FLT uptake changes, there were 16 responders and 14 nonresponders. ^{18}F-FLT tumor uptake decreased by 46% ± 14% in responders but increased by 20% ± 52% in nonresponders ($P = 0.001$). Median OS for responders based on ^{18}F-FLT criteria was 3.3 times as long as that of the nonresponders (12.5 vs. 3.8 mo, $P < 0.001$).

With the observation that there were small ^{18}F-FLT tumor uptake reductions at 2 wk, even in patients with poor outcomes, attention was paid to changes of ^{18}F-FLT tumor uptake between 2 and 6 wk. These changes yielded a significant correlation with patient outcome. Receiver-operating-characteristic analysis revealed an optimal threshold value of +7%, with lower values corresponding to longer patient survival (area under the curve, 0.779; $P =$ 0.017; sensitivity and specificity, 82% and 70%, respectively). Kaplan–Meier analysis resulted in a significant survival prediction (Log rank $P < 0.001$; Fig. 3) using this threshold.

^{18}F-FLT uptake changes were also predictive of PFS: $P = 0.019$ at 2 wk, $P < 0.001$ at 6 wk, and $P = 0.006$ comparing ^{18}F-FLT uptake changes between 2 and 6 wk (Fig. 4).

Response Assessment by MRI

Response by MRI was evaluated at approximately 6 wk (5.9 ± 2.7) after starting treatment based on RANO criteria and was available for 29 patients. By MRI criteria, 9 patients were classified as responders (31%). Seven of these had a PR, and 2 had a CR. Thirteen patients had stable disease (45%), and 7 had progressive disease (PD) (24%). MRI response was predictive of OS and PFS ($P = 0.01$ and 0.001, respectively). Median OS for responders based on MRI criteria was 1.4 times as long as that of nonresponders (12.9 vs. 9.0 mo, $P = 0.05$).

^{18}F-FLT PET Changes, Compared with Other Clinical Predictors

Multiple clinical variables were tested by univariate and multivariate analyses (Table 3). By univariate analysis, survival was better if patients had fewer recurrences. Patients' age, baseline KPS, and dexamethasone treatment were not predictive of survival.

Changes in ^{18}F-FLT tumor uptake from baseline to 2 wk, baseline to 6 wk, and 2 to 6 wk were all predictive of survival ($P < 0.001$). However, ^{18}F-FLT tumor uptake changes at 6 wk provided the highest hazard ratio (HR; 7.869 vs. 5.416 for baseline to 2 wk and 5.739 for 2–6 wk).

Response by MRI was also predictive of survival ($P = 0.016$). By multivariate analysis, change of tumor ^{18}F-FLT SUV from baseline to 6 wk was the most significant predictor of OS ($P < 0.001$; HR, 10.051).

Similarly, longer PFS was predicted if patients had fewer prior recurrences. Patients' age, baseline KPS, and dexamethasone treatment were not predictive of PFS. ^{18}F-FLT PET responses at 2 wk, 6 wk, and from 2 to 6 wk and MRI response were all predictive of PFS (Table 3). By multivariate analysis, ^{18}F-FLT PET assessment at 6 wk was the most significant predictor of PFS ($P = 0.001$; HR, 5.636).

DISCUSSION

We report the first completed prospective study of metabolic response with ^{18}F-FLT PET in patients with recurrent high-grade glioma on bevacizumab therapy. The current study expands on the prior pilot study (20) of a smaller set of 19 patients. Now we provide complete survival data of 30 patients and include updated MRI data at 6 wk based on RANO criteria.

First, this study demonstrates that ^{18}F-FLT uptake in the early phase of antiangiogenic treatment is indeed predictive of OS in patients with recurrent high-grade glioma. ^{18}F-FLT uptake changes from both baseline to 2 wk and base-line to 6 wk after starting treatment are predictive of OS ($P < 0.001$). Second, this study shows that changes of ^{18}F-FLT uptake from baseline to 6 wk (HR, 7.869) are stronger predictors of OS than changes at 2 wk (HR, 5.416). Changes in ^{18}F-FLT tumor uptake at 6 wk stratifies patients into 2 subgroups, ^{18}F-FLT responders (16/30, 53%) and nonresponders (14/30, 47%). ^{18}F-FLT responders survived for 12.5 mo, which is 3.3 times longer than the 3.8-mo survival for nonresponders ($P < 0.001$). Third, the current study also demonstrates the significant power of ^{18}F-FLT for predicting PFS ($P = 0.019$ at 2 wk and $P < 0.001$ at 6 wk). Fourth, absolute ^{18}F-FLT uptake values at any time point are not predictive of survival. Finally, we compared metabolic responses by ^{18}F-FLT with MRI response at 6 wk based on RANO criteria. MRI at 6 wk identifies 9 responders (31%; 7 PR and 2 CR), 13 patients with stable disease (45%), and 7 patients with PD (24%) and is predictive of OS. However, median OS, although being 3.3 times longer for ^{18}F-FLT PET responders than for nonresponders, is only 1.4 times longer for MRI responders than for MRI nonresponders (12.9 vs. 9.0 mo, $P = 0.05$). Further, multivariate analysis identifies ^{18}F-FLT PET at 6 wk as the most significant predictor for OS ($P < 0.001$; HR, 10.051) and PFS ($P = 0.001$; HR, 5.636).

There were discrepancies in response assessments between MRI and PET at 6 wk in 8 patients. MRI interpretation at 6 wk was based on RANO criteria (14). However, as the aim of the current study was to compare survival predictions of ^{18}F-FLT PET and MRI at 6 wk, the 4-wk sustained response requirement by RANO for MRI-based responses was not applied here. One patient identified by MRI as PR was an ^{18}F-FLT PET nonresponder (patient 9, Table 2). This patient died 2.8 mo after starting the treatment. Conversely, there were 7 patients who were ^{18}F-FLT PET responders but non-responders by MRI (6 stable disease, 1 PD). The median OS for these 7 patients was 12.3 mo (range, 10.4–19.5 mo). Thus, rather than detecting treatment failure earlier than MRI (as reported for O-(2-^{18}F-fluoroethyl)-L-tyrosine recently), ^{18}F-FLT PET appears to identify treatment responders earlier than MRI (24).

At the onset of treatment, between the baseline and first follow-up scan at 2 wk, a reduction in ^{18}F-FLT tumor uptake from the baseline value was observed in essentially all patients (Fig. 2). For the subgroup of patients with greater than 12-mo survival ($n = 11$), there was a median SUV reduction of 37% from baseline after 2 wk and 47% after 6 wk. Even in those with less than 12-mo survival ($n = 19$), there was a median SUV reduction of 22% from baseline after the first 2 wk of treatment. However, in this group of patients with less than 12-mo survival, this early median SUV decrease was followed by a rebound of 33% at the second follow-up ^{18}F-FLT scan at 6 wk after starting treatment, bringing the median SUV close to the baseline value.

It has been observed that antiangiogenic agents can produce a rapid decrease in contrast enhancement in MRI that occurs within days of initiation of treatment (15,25). This decrease is considered at least in part a result of reduced vascular permeability to contrast agents rather than a true antitumor effect because MRI contrast changes were not predictive of survival (13–15). It is possible that the initial decreases in ^{18}F-FLT uptake as universally observed in our study can be similarly attributed in part to bevacizumab's effect on vascular permeability. However, the strong predictive power of ^{18}F-FLT changes demonstrated in our study in OS and PFS argues that ^{18}F-FLT changes do reflect a true response to the antineoplastic effect of the treatment.

Bevacizumab causes normalization of vascular architecture, leading to an improved blood flow to the tumor (26). This paradoxic effect on tumor vasculature aids in the delivery of concomitantly administered chemotherapeutic agents. Furthermore, it reduces vasogenic edema, allowing for a reduction or discontinuation of corticosteroids (27). Finally, bevacizumab effectively blocks new blood vessel formation, curbing tumor proliferation to the diffusion limits of existing capillaries (28,29). Our study demonstrated a median OS of 10.3 mo in patients with recurrent high-grade glioma, consistent with previously published studies (5,9,10). The improvement in OS strongly suggests that in addition to the blood–brain barrier restoration effect, bevacizumab has a true antineoplastic effect in responders, leading to longer OS.

With the advance of targeted therapies, which also can be associated with significant toxicity and side effects, a non-invasive and early evaluation of treatment response that is predictive of OS becomes critically important. A study of apparent diffusion coefficient histograms in recurrent glioblastoma patients before bevacizumab treatment was reported to be predictive of 6-mo PFS (30). No data on OS were reported in that study. Vascular normalization was hypothesized to be predictive of outcome in a study of recurrent glioblastoma patients on cediranib treatment, an oral pan–vascular endothelial growth factor receptor tyrosine kinase inhibitor (30). Three parameters—that is, changes in vascular permeability and flow (K^{trans}), microvessel volume, and the change of circulating type-IV collagen intravenous levels—were combined into a vascular normalization index, which was found to be predictive of PFS and OS (31).

^{18}F-FLT is a thymidine analog that is transported into tumor cells via nucleoside transporters and is subsequently phosphorylated by thymidine kinase 1 to ^{18}F-FLT 5-phosphate (19). Although ^{18}F-FLT is not incorporated into DNA, its uptake correlates with tumor tissue proliferation as determined by Ki-67 antibody staining (32,33). Thus, ^{18}F-FLT uptake reflects the proliferative activity of cells. The current study shows that changes in tumor ^{18}F-FLT uptake could be used to predict patient survival. This is clinically relevant because these predictions allow for the early stratification of patients into responders and nonresponders, thereby allowing the discontinuation of ineffective treatments in nonresponding patients.

One limitation of our study is the absence of kinetic data. Kinetic modeling of ^{18}F-FLT in brain tumors showed that ^{18}F-FLT uptake in tumor tissues seems to be predominantly due to elevated transport and net influx (34). Further, kinetic studies demonstrated a good correlation between the net influx rate constant and ^{18}F-FLT uptake, suggesting that simple semiquantitative analysis of SUV might be sufficient for clinical applications (35). This notion was supported by several preclinical and clinical studies when reductions in ^{18}F-FLT uptake after the start of treatment correlated with therapeutic effects in experimental gliomas in animal studies (36,37). ^{18}F-FLT PET was used to monitor disease status and to direct treatment in a patient with glioblastoma, and ^{18}F-FLT uptake ratios and kinetic parameters provided concordant information (38). We have also used kinetic models and have reported the results previously (39). Patients were stratified into 3 groups based on survival time— less than 6 mo, 6–12 mo, and greater than 12 mo. None of the rate constants was significantly different between the groups. However, a significant decrease in SUV was seen in long-term survivors but not in short-term survivors. Significant correlations were again found between SUV and both the rate constant and the influx rate. Thus, the use of the semi-quantitative SUV approach for assessing tumor responses is entirely justified.

CONCLUSION

Although future larger validation studies are needed, the present data suggest that ^{18}F-FLT PET provides a powerful prognostic tool in recurrent high-grade glioma patients treated with bevacizumab.

Acknowledgments

References

1. Wong ET, Hess KR, Gleason MJ, et al. Outcomes and prognostic factors in recurrent glioma patients enrolled onto phase II clinical trials. J Clin Oncol. 1999; 17:2572–2578. [PubMed: 10561324]

2. Wen PY, Kesari S. Malignant gliomas in adults. N Engl J Med. 2008; 359:492–507. [PubMed: 18669428]

3. Hicklin DJ, Ellis LM. Role of the vascular endothelial growth factor pathway in tumor growth and angiogenesis. J Clin Oncol. 2005; 23:1011–1027. [PubMed: 15585754]

4. Ferrara N, Hillan KJ, Novotny W. Bevacizumab (Avastin), a humanized anti-VEGF monoclonal antibody for cancer therapy. Biochem Biophys Res Commun. 2005; 333:328–335. [PubMed: 15961063]

5. Vredenburgh JJ, Desjardins A, Herndon JE, et al. Bevacizumab plus irinotecan in recurrent glioblastoma multiforme. J Clin Oncol. 2007; 25:4722–4729. [PubMed: 17947719]

6. Raymond E, Fabbro M, Boige V, et al. Multicentre phase II study and pharmacokinetic analysis of irinotecan in chemotherapy-naive patients with glioblastoma. Ann Oncol. 2003; 14:603–614. [PubMed: 12649109]

7. Prados MD, Lamborn K, Yung WKA, et al. A phase 2 trial of irinotecan (CPT-11) in patients with recurrent malignant glioma: a North American Brain Tumor Consortium study. Neuro-oncol. 2006; 8:189–193. [PubMed: 16533878]

8. Ballman KV, Buckner JC, Brown PD, et al. The relationship between six-month progression-free survival and 12-month overall survival end points for phase II trials in patients with glioblastoma multiforme. Neuro-oncol. 2007; 9:29–38. [PubMed: 17108063]

9. Narayana A, Kelly P, Golfinos J, et al. Antiangiogenic therapy using bevacizumab in recurrent high-grade glioma: impact on local control and patient survival. J Neurosurg. 2009; 110:173–180. [PubMed: 18834263]

10. Friedman HS, Prados MD, Wen PY, et al. Bevacizumab alone and in combination with irinotecan in recurrent glioblastoma. J Clin Oncol. 2009; 27:4733–4740. [PubMed: 19720927]

11. Macdonald DR, Cascino TL, Schold SC, Cairncross JG. Response criteria for phase-II studies of supratentorial malignant glioma. J Clin Oncol. 1990; 8:1277–1280. [PubMed: 2358840]

12. Levivier M, Becerra A, DeWitte O, Brotchi J, Goldman S. Radiation necrosis or recurrence. J Neurosurg. 1996; 84:148–149. [PubMed: 8613825]

13. van den Bent MJ, Vogelbaum MA, Wen PY, Macdonald DR, Chang SM. End point assessment in gliomas: novel treatments limit usefulness of classical Macdonald's criteria. J Clin Oncol. 2009; 27:2905–2908. [PubMed: 19451418]

14. Wen PY, Macdonald DR, Reardon DA, et al. Updated response assessment criteria for high-grade gliomas: Response Assessment in Neuro-Oncology Working Group. J Clin Oncol. 2010; 28:1963–1972. [PubMed: 20231676]

15. Ellingson B, Cloughesy T, Lai A, Nghiemphu P, Mischel P, Pope W. Quantitative volumetric analysis of conventional MRI response in recurrent glioblastoma treated with bevacizumab. Neuro-Oncology. 2011; 13:401–409. [PubMed: 21324937]

16. Alavi JB, Alavi A, Chawluk J, et al. Positron emission tomography in patients with glioma: a predictor of prognosis. Cancer. 1988; 62:1074–1078. [PubMed: 3261622]

17. Wong TZ, van der Westhuizen GJ, Coleman RE. Positron emission tomography imaging of brain tumors. Neuroimaging Clin N Am. 2002; 12:615–626. [PubMed: 12687915]

18. Ricci PE, Karis JP, Heiserman JE, Fram EK, Bice AN, Drayer BP. Differentiating recurrent tumor from radiation necrosis: time for re-evaluation of positron emission tomography? AJNR. 1998; 19:407–413. [PubMed: 9541290]

19. Shields AF, Grierson JR, Dohmen BM, et al. Imaging proliferation in vivo with [F-18]FLT and positron emission tomography. Nat Med. 1998; 4:1334–1336. [PubMed: 9809561]

20. Chen W, Delaloye S, Silverman DHS, et al. Predicting treatment response of malignant gliomas to bevacizumab and irinotecan by imaging proliferation with [F-18] fluorothymidine positron emission tomography: a pilot study. J Clin Oncol. 2007; 25:4714–4721. [PubMed: 17947718]

21. Blocher A, Kuntzsch M, Wei R, Machulla HJ. Synthesis and labeling of 5′-O-(4,4′-dimethoxytrityl)-2,3′-anhydrothymidine for [F-18]FLT preparation. J Radioanal Nucl Chem. 2002; 251:55–58.

22. Kaplan EL, Meier P. Nonparametric-estimation from incomplete observations. J Am Stat Assoc. 1958; 53:457–481.

23. Cox DR. Regression models and life-tables. J R Stat Soc, B. 1972; 34:187–202.

24. Hutterer M, Nowosielski M, Putzer D, et al. O-(2-^{18}F-Fluoroethyl)-L-tyrosine PET predicts failure of antiantiogenic treatment in patients with recurrent high-grade glioma. J Nucl Med. 2011; 52:856–864. [PubMed: 21622893]

25. Port RE, Bernstein LJ, Barboriak DP, Xu L, Roberts TPL, van Bruggen N. Noncompartmental kinetic analysis of DCE-MRI data from malignant tumors: application to glioblastoma treated with bevacizumab. Magn Reson Med. 2010; 64:408–417. [PubMed: 20665785]

26. Gonzalez J, Kumar AJ, Conrad CA, Levin VA. Effect of bevacizumab on radiation necrosis of the brain. Int J Radiat Oncol Biol Phys. 2007; 67:323–326. [PubMed: 17236958]

27. Jain RK. Normalization of tumor vasculature: an emerging concept in antiangiogenic therapy. Science. 2005; 307:58–62. [PubMed: 15637262]

28. Dvorak HF. Vascular permeability factor/vascular endothelial growth factor: a critical cytokine in tumor angiogenesis and a potential target for diagnosis and therapy. J Clin Oncol. 2002; 20:4368–4380. [PubMed: 12409337]

29. de Groot JF, Fuller G, Kumar AJ, et al. Tumor invasion after treatment of glioblastoma with bevacizumab: radiographic and pathologic correlation in humans and mice. Neuro-oncol. 2010; 12:233–242. [PubMed: 20167811]

30. Pope WB, Kim HJ, Huo J, et al. Recurrent glioblastoma multiforme: ADC histogram analysis predicts response to bevacizumab treatment. Radiology. 2009; 252:182–189. [PubMed: 19561256]

31. Sorensen AG, Batchelor TT, Zhang WT, et al. A "vascular normalization index" as potential mechanistic biomarker to predict survival after a single dose of cediranib in recurrent glioblastoma patients. Cancer Res. 2009; 69:5296–5300. [PubMed: 19549889]

32. Chen W, Cloughesy T, Kamdar N, et al. Imaging proliferation in brain tumors with F-18-FLT PET: comparison with F-18-FDG. J Nucl Med. 2005; 46:945–952. [PubMed: 15937304]

33. Ullrich R, Backes H, Li H, et al. Glioma proliferation as assessed by 3′-fluoro-3′-deoxy-L-thymidine positron emission tomography in patients with newly diagnosed high-grade glioma. Clin Cancer Res. 2008; 14:2049–2055. [PubMed: 18381944]

34. Jacobs AH, Thomas A, Kracht LW, et al. ^{18}F-fluoro-L-thymidine and ^{11}C-methyl-methionine as markers of increased transport and proliferation in brain tumors. J Nucl Med. 2005; 46:1948–1958. [PubMed: 16330557]

35. Schiepers C, Chen W, Dahlbom M, et al. ^{18}F-fluorothymidine kinetics of malignant brain tumors. Eur J Nucl Med Mol Imaging. 2007; 34:1003–1011. [PubMed: 17295039]

36. Rueger MA, Ameli M, Li H, et al. [18F]FLT PET for non-invasive monitoring of early response to gene therapy in experimental gliomas. Mol Imaging Biol. 2011; 13:547–557. [PubMed: 20563754]

37. Jacobs AH, Rueger MA, Winkeler A, et al. Imaging-guided gene therapy of experimental gliomas. Cancer Res. 2007; 67:1706–1715. [PubMed: 17308112]

38. Galldiks N, Kracht LW, Burghaus L, et al. Patient-tailored, imaging-guided, long-term temozolomide chemotherapy in patients with glioblastoma. Mol Imaging. 2010; 9:40–46. [PubMed: 20128997]

39. Schiepers C, Dahlbom M, Chen W, et al. Kinetics of 3′-deoxy-3′-^{18}F-fluorothymidine during treatment monitoring of recurrent high-grade glioma. J Nucl Med. 2010; 51:720–727. [PubMed: 20395318]
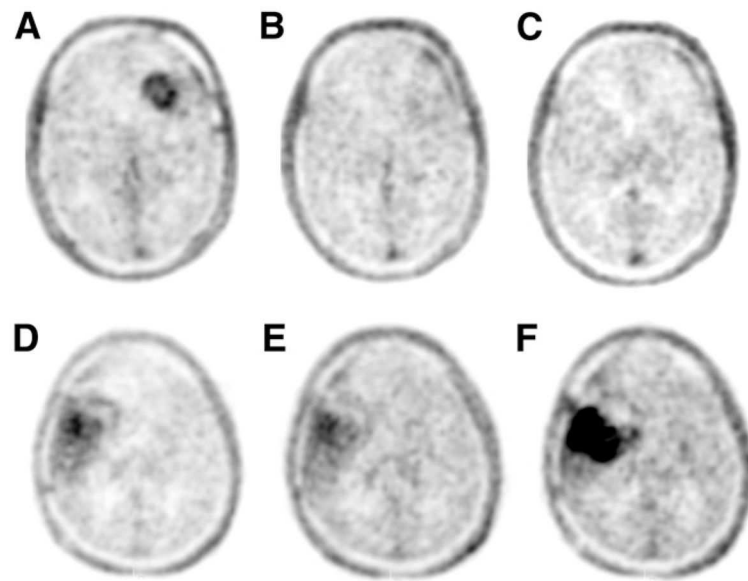
FIGURE 1.
^{18}F-FLT PET at baseline, 2 wk, and 6 wk for responding patient (A, B, and C, respectively, patient 25, Table 2) and non-responding patient (D, E, and F, respectively, patient 9, Table 2).
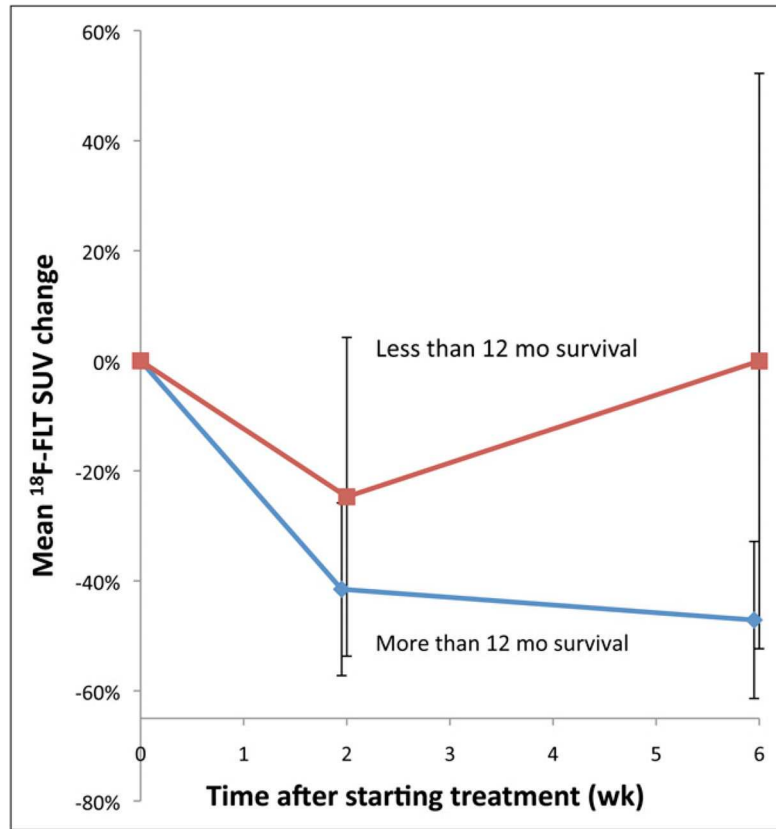
FIGURE 2.
Mean ^{18}F-FLT SUV changes for patients as function of time for patients with more or less than 12-mo survival. Initial drop of SUV is universally observed.
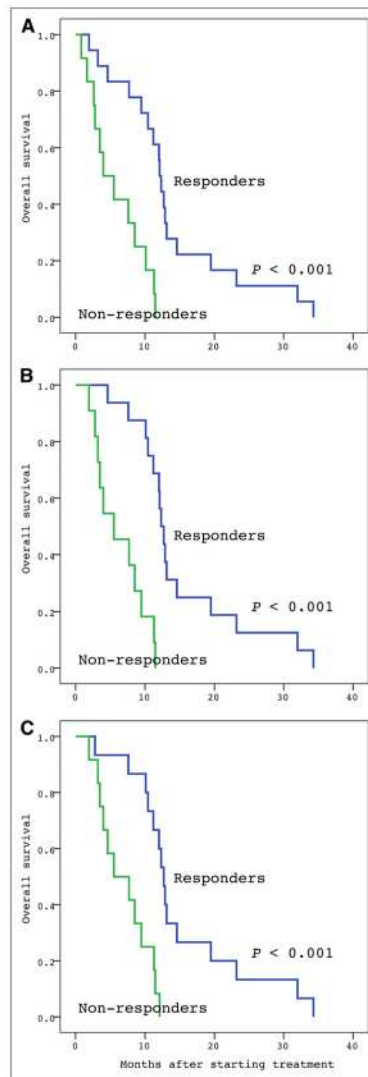
FIGURE 3.
OS Kaplan–Meier curves separated by ^{18}F-FLT PET based on baseline to 2 wk (A), baseline to 6 wk (B), and 2–6 wk (C) response criteria.
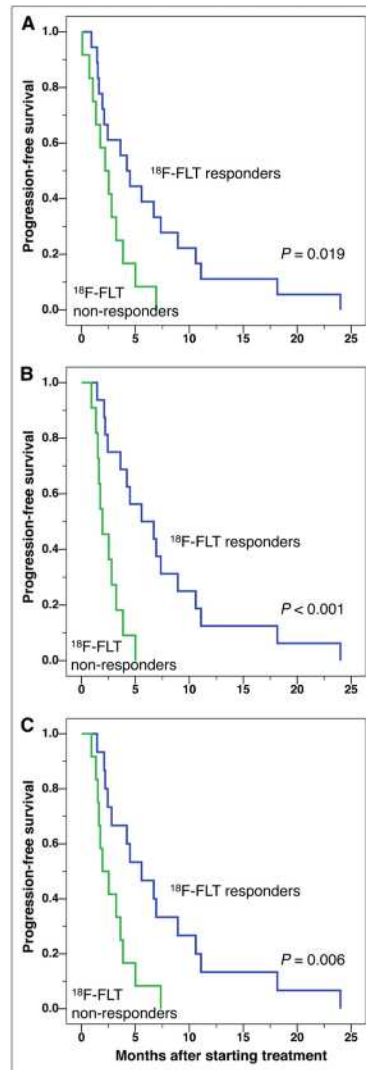
FIGURE 4.
PFS Kaplan–Meier curves separated by ^{18}F-FLT PET based on baseline to 2 wk (A),
baseline to 6 wk (B), and 2–6 wk (C) response criteria.

TABLE 1

Patient Characteristics

Characteristic	n
Sex	
Female	12
Male	18
Tumor grade	
Grade III	6
Grade IV	24
KPS	
70–80	13
90–100	17
No. of recurrences	
1–2	24
3–4	5
5	1
Dexamethasone treatment	
Absence	12
Presence	18

Median age of patients was 58 y, and age range was 26–78 y.

TABLE 2

Patient Characteristics, Tumor ^{18}F-FLT Uptake, and OS ($n = 30$)

Patient no.	Sex	Age (y)	Diagnosis	SUV						Response (6 wk)			
				Baseline	2 wk after treatment start	6 wk after treatment start	Change at 2 wk	Change at 6 wk	Change between 2 and 6 wk	^{18}F-FLT PET	MRI*	PFS (mo)	OS (mo)
1	F	38	AA	0.74	0.59	0.78	−20%	+5%	+32%	No	SD	5.0	8.5
2	M	78	GBM	1.57	2.28	ND	45%	NA	NA	No	PD	0.5	0.8
3	M	64	GBM	0.88	0.68	0.63	−23%	−28%	−7%	Yes	PR	2.2	7.6
4	F	45	GBM	0.74	0.82	1.67	+11%	+126%	+104%	No	SD	1.7	11.3
5	M	37	GBM	1.56	1.30	1.39	−17%	+11%	+7%	No	SD	3.8	4.0
6	M	65	AA	0.83	0.44	0.56	−47%	−33%	+27%	Yes	†	3.6	4.6
7	M	65	AMG	0.64	0.50	ND	−22%	NA	NA	No	PD	0.7	2.6
8	F	61	GBM	1.69	1.16	1.15	−31%	−32%	−1%	Yes‡	SD‡	4.5	13.1
9	M	69	GBM	0.45	0.45	0.39	0%	−13%	−13%	No‡	PR‡	2.8	2.8
10	M	26	GBM	0.75	0.74	1.08	−1%	+44%	+46%	No	SD	3.2	11.5
11	F	65	GBM	0.69	0.60	1.20	−13%	+74%	+100%	No	SD	2.5	3.5
12	F	35	GBM	0.72	0.33	0.35	−54%	−51%	+6%	Yes‡	PD‡	2.1	10.4
13	F	62	GBM	0.59	0.37	0.39	−37%	−34%	+5%	Yes	PR	8.9	23.2
14	M	28	AA	0.81	0.46	0.62	−43%	−23%	+35%	No	PD	1.5	7.7
15	F	68	GBM	1.34	1.04	ND	−22%	NA	NA	No	PD	1.1	1.6
16	F	47	GBM	2.35	1.42	1.33	−40%	−43%	−6%	Yes‡	SD‡	5.6	12.7
17	F	54	GBM	1.22	0.61	0.65	−50%	−47%	+7%	Yes	PR	7.3	12.1

| Patient no. | Sex | Age (y) | Diagnosis | SUV | | | | | | Response (6 wk) | | | |
				Baseline	2 wk after treatment start	6 wk after treatment start	Change at 2 wk	Change at 6 wk	Change between 2 and 6 wk	18F-FLT PET	MRI[*]	PFS (mo)	OS (mo)
18	M	58	GBM	4.79	1.78	5.24	−63%	+9%	+194%	No	SD	1.6	3.2
19	M	46	GBM	1.81	0.82	0.62	−55%	−66%	−24%	Yes[‡]	SD[‡]	2.4	11.2
20[‡]	M	50	AA	0.22	0.22	1.22	−79%	−56%[¶]	+109%	No[¶]	SD	0.9	1.9
21	M	70	GBM	0.91	0.63	0.42	−31%	−54%	−33%	Yes	PR	6.7	12.9
22	M	66	GBM	0.94	0.62	0.51	−34%	−46%	−18%	Yes[‡]	SD[‡]	11.1	12.3
23	M	47	GBM	0.38	0.19	0.19	−50%	−50%	0%	Yes	CR	18.2	34.3
24	F	58	GBM	1.01	0.89	1.60	−12%	+58%	+80%	No	SD	1.3	5.5
25	M	76	GBM	1.36	0.25	0.22	−82%	−84%	−12%	Yes	CR	24.0	32.0
26	M	68	GBM	2.02	1.74	1.26	−14%	−38%	−28%	Yes	PR	6.9	10.1
27	F	37	GBM	1.32	0.95	0.89	−28%	−33%	−6%	Yes	PR	10.6	14.6
28	M	37	AA	0.86	0.51	0.88	−41%	+2%	+73%	No	PD	1.9	9.5
29	M	57	GBM	0.66	0.48	0.35	−27%	−47%	−27%	Yes[‡]	SD[‡]	4.2	19.5
30	F	41	GBM	1.99	1.06	1.01	−47%	−49%	−5%	Yes[‡]	PD[‡]	1.4	12.0

[*] This being MRI evaluation at 6 wk, no 4-wk sustained response requirement for responders based on RANO (14) was taken into consideration for this evaluation.

[†] Follow-up MRI not available for evaluation.

[‡] Mismatch between MRI and PET response assessment.

[¶] Patient developed second lesion after 2 wk.

AA= anaplastic astrocytoma; SD = stable disease; GBM = glioblastoma multiforme; ND = not done; NA = not applicable; AMG = anaplastic mixed glioma.

NIH-PA Author Manuscript

NIH-PA Author Manuscript

NIH-PA Author Manuscript

TABLE 3

Cox Regression Analysis of OS and PFS of Predictive Factors

Predictive factor	OS				PFS			
	Univariate		Multivariate		Univariate		Multivariate	
	P	HR	*P*	HR	*P*	HR	*P*	HR
Age	0.939				0.325			
No. of recurrences	0.001	2.243	0.645		0.001	2.044	0.267	
Baseline KPS	0.06				0.915			
Dexamethasone treatment	0.176				0.731			
Tumor size change by MRI	0.016	3.220	0.382		0.003	4.151	0.054	
Lack of ^{18}F-FLT reduction, 0–2 wk	0.001	5.416	0.795		0.024	2.590	0.264	
Lack of ^{18}F-FLT reduction, 0–6 wk	<0.001	7.869	<0.001	10.051	0.001	5.225	0.001	5.636
Lack of ^{18}F-FLT increase, 2–6 wk	0.001	5.739	0.674		0.009	3.197	0.833	